International Journal of Computer Information Systems and Industrial Management Applications
ISSN 2150-7988 Volume 18 (2026) pp. 1-18
© Cerebration Science Publishing
https://doi.org/10.70917/ijcisim-2026-0073
Article

Improvement of Clothing Structure Design and Wearing Comfort Based on Jacobi Matrix Optimization Algorithm

Linqian Ma *

Graduate School of Design, Tongmyong University, Busan 48520, Korea; mlq723511722@126.com

Abstract: Clothing structure design is a key link in the clothing manufacturing process, and the traditional design methods rely on the experience and skills of designers. With the development and application of digital technology in the apparel industry, it has greatly promoted the innovation and development of apparel manufacturing. In this paper, we combine the depth estimation and vision controller methods to construct an image Jacobi matrix to realize the control of the hand-eye mapping relationship of the robot's visual servo, which represents the mapping relationship between the robot's joint speed to the end speed. Using Kalman filtering algorithm, the image Jacobi matrix to be estimated is used as the system state to estimate the system state, so as to achieve the control of the stitch and displacement of the garment sewing, and, at the same time, capture the visual information contained in the garment to optimize the design of the garment structure. For the optimized designed garments using the Jacobi matrix, 4# has the highest mean comfort rating of 4.5 and above. The mean value of satisfaction evaluation for ease of movement and overall comfort of the optimized garment went up to 4. It is evident that the overall comfort of the garment optimized by the image Jacobi matrix algorithm has been significantly improved.

Keywords: Depth estimation; vision controller; image Jacobi matrix; Kalman filtering; garment structural design

1. Introduction

Clothing, which began as simple leaf coverings, has evolved far beyond its practical functions to embody people's beliefs and values. The development of clothing has become an art form, blending material elements with spiritual ones to provide aesthetic enjoyment [1-2]. In the field of clothing design, innovation is indispensable, whether in ready-to-wear or haute couture. Only through continuous innovation can one create their own unique clothing. As a designer, finding the right creative direction requires constant practice and accumulation [3-4]. Designers draw their practice and accumulation from the details of daily life; only life can continuously inspire designers.

Modern clothing engineering consists of three major components: style design, structural design, and process design. Structural design is a crucial component of clothing engineering [5]. Through structural design, three-dimensional clothing shapes are converted and decomposed into two-dimensional graphics, enabling precise adjustments to achieve an ideal, flattering silhouette. Additionally, structural design provides precise and reasonable patterns for sewing and processing—these patterns serve as essential references for cutting and sewing the various components of clothing. Clothing structural design serves as a bridge between clothing style design and process design, acting as an extension of style design and the foundation of process design, playing a pivotal role in connecting the two [6-8]. The results of clothing structural design directly impact the functionality and aesthetics of clothing.

As a science studying the interaction and optimization between humans and other elements, ergonomics aims to enhance the efficiency and safety of human activities while reducing fatigue and discomfort associated with such activities [9]. Therefore, clothing designers should recognize the importance of ergonomics, deeply understand the dynamic relationship between clothing and the human body, and use scientific design methods to enhance the wearing experience of clothing and make it adaptable to different physical activities [10-12]. The emergence of new materials and technologies has

Copyright: © 2026 by the authors

opened up broader development prospects for modern clothing design. The application of these technologies and materials has enhanced the functionality of clothing and, through data integration technology, strengthened its interactivity [13-15]. Although technological advancements have opened new possibilities for clothing design, how to effectively integrate these technologies into the framework of ergonomics to design clothing that both adheres to ergonomic principles and meets modern functional requirements remains a critical issue that designers must address urgently.

The Jacobian matrix algorithm is an iterative numerical method used to solve nonlinear systems of equations, approximating the roots of the problem by linearizing the system of equations, and can be applied in engineering. Reference [16] addresses the issue of eigenvalues and their corresponding eigenvectors being arranged in a disordered manner in the traditional Jacobian algorithm, proposing an improved Jacobian algorithm that can obtain eigenvalues and eigenvectors in descending order. Reference [17] derives various properties of similarity transformations between Jacobian matrices and proves these properties through simple matrix calculus.

Modern clothing design is moving toward smarter, more sophisticated, and more convenient directions. Reference [18] proposes a new interactive design method for custom clothing oriented toward sustainable fashion. It estimates human body dimensions while meeting consumers' ergonomic requirements, generates design schemes based on a GA model, and evaluates clothing fit through a probabilistic neural network. This method was validated in an actual application case of customizing casual pants. Literature [19] employs parametric design for clothing and implements an automatic pattern generation method based on Python. This design method offers high accuracy and comfort while reducing resource consumption, contributing to the sustainable development of the clothing industry. Literature [20] emphasizes the connection between morphological contours and human body measurements, designing and implementing a digital clothing design technology in the three-dimensional pattern-making process. This technology controls the fit of three-dimensional clothing by adjusting human body morphology to determine ease. Literature [21] describes each clothing modeling element based on the construction of three-dimensional virtual human models and ease models, combining them into two interconnected sub-models to achieve virtual clothing model design. Literature [22] analyzes the application characteristics and issues of three-dimensional clothing virtual design technology from the perspective of its development and trends, exploring ways to promote the comprehensive integration of the talent supply chain and the fashion industry chain, as well as the cultivation of application-oriented, composite talent.

In this paper, the depth estimation method is used to calculate the value of the image Jacobi matrix at the current moment according to the camera imaging model, and the robot's moving speed is controlled by the Jacobi matrix. Combining the robot Jacobi matrix and the visual projection mapping transformation equation, the relationship between the robot joint motion speed and the image feature motion speed is obtained, so as to establish the mapping model from the robot joint motion space to the image feature space. On this basis, the Kalman wave theory is introduced for online estimation of the system state to achieve continuous matching in the image and tracking of the robot. The designed optimization model is used to control the stitching and displacement in the sewing process of the garment, to identify the garment style, to carry out the visual evaluation of the garment, and to complete the optimization and transformation of the garment design. The comfort and satisfaction assessment of the garment samples are tested through simulation experiments to further optimize the garment structure design.

2. Clothing Structure Design Based on Jacobi Matrix Optimization Algorithm

2.1. Depth Estimation Method and Visual Controller Design

2.1.1. Depth Estimation Methods

The camera eye is mounted on the hand as shown in Fig. 1, assuming that p_1, p_2 are two points on the surface of the object, whose coordinates under the camera coordinate system are $p_1 = (x_1, y_1, z_1), p_2 = (x_2 y_2, z_2)$, l_1 is the distance between the two points p_1, p_2, the coordinates of the points p_1, p_2 in the camera coordinate system are unknown, but the distance l between these two points is known. It is obtained based on the geometric relationship:

$$l = \sqrt{(x_1 - x_2)^2 + (y_1 - y_2)^2 + (z_1 - z_2)^2} \tag{1}$$

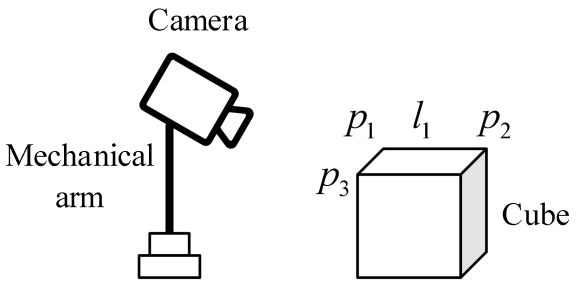

Figure 1. Shows a robot model with eyes on the hand.

Assume that the coordinates of the two points p_1, p_2 in the pixel plane are $(u_1, v_1), (u_2, v_2)$, which can be obtained from the camera imaging model:

$$t\begin{bmatrix} u_1 \\ v_1 \end{bmatrix} = t\begin{bmatrix} f\frac{x_1}{z_1} + u_0 \\ f\frac{y_1}{z_1} + v_0 \end{bmatrix} \tag{2}$$

$$t\begin{bmatrix} u_2 \\ v_2 \end{bmatrix} = t\begin{bmatrix} f\frac{x_2}{z_2} + u_0 \\ f\frac{y_2}{z_2} + v_0 \end{bmatrix} \tag{3}$$

Simplify the above formula:

$$t\begin{bmatrix} u_1^{'} \\ v_1^{'} \end{bmatrix} = t\begin{bmatrix} u_1 - u_0 \\ v_1 - v_0 \end{bmatrix} \tag{4}$$

$$t\begin{bmatrix} u_2^{'} \\ v_2^{'} \end{bmatrix} = t\begin{bmatrix} u_2 - u_0 \\ v_2 - v_0 \end{bmatrix} \tag{5}$$

$$t\begin{bmatrix} x_1 \\ y_1 \end{bmatrix} = \frac{1}{f}\begin{bmatrix} u_1^{'} z_1 \\ v_1^{'} z_1 \end{bmatrix} \tag{6}$$

$$t\begin{bmatrix} x_2 \\ y_2 \end{bmatrix} = \frac{1}{f}\begin{bmatrix} u_2^{'} z_2 \\ v_2^{'} z_2 \end{bmatrix} \tag{7}$$

Substituting Eq. (7) into Eq. (1) yields:

$$\begin{aligned} &(u_1^{'} + v_1^{'} + f)z_1^2 + (u_2^{'} + v_2^{'} + f)z_2^2 \\ &-2(u_1^{'}u_2^{'} + v_1^{'}v_2^{'} + f)z_1 z_2 = (fl)^2 \end{aligned} \tag{8}$$

Usually the surface of the object is in parallel with the camera, and the depth values of each feature point can be considered equal in magnitude, i.e., $z_1 = z_2$. Equation (8) can be simplified:

$$((u_1 - u_2)^2 + (v_1 - v_2)^2) \times z^2 = f^2 l^2 \tag{9}$$

The value of depth z is obtained from equation (9):

$$z = fl / \sqrt{(u_1 - u_2)^2 + (v_1 - v_2)^2} \tag{10}$$

Combining Eq. (5) and Eq. (7) yields:

$$x = \frac{z}{f}(u - u_0)$$
$$y = \frac{z}{f}(v - v_0) \tag{11}$$

The size of the depth z can be solved according to equation (9) when the geometry of the object is known. The value of x, y can be solved by Eq. (11), and the value of the image Jacobi matrix at the current moment can be calculated by substituting the solved z, x, y into Eq. (1). The current moment robot end velocity magnitude can be solved by equation (12).

$$v = k_p J_p e \tag{12}$$

where k_p is the scale factor, J_p is the image Jacobi matrix, and e is the rate of change of image features.

In robotics, the robot Jacobi matrix is often used to relate the robot end velocities to the velocities at each joint of the robot, as shown in equation (13):

$$^0v = {}^0J(\theta)\theta \tag{13}$$

where $J(\theta)$ is the robot Jacobi matrix, which can be solved based on the current joint angles of the robot and the DH parameters [23].

The velocity at the end of the robot can be solved by Eq. (12), and the velocity at each joint of the robot can be solved by substituting the velocity at the end of the robot into Eq. (13), as shown in Eq. (14). Integrate the speed of each joint to obtain the size of the angle value of the robot for that rotation, and send the angle value down to the controller to drive the robot to move to the next position:

$$\theta = J(\theta)^{-1} v \tag{14}$$

2.1.2. Visual Controller Design

The robot motion is realized based on the GALIL motion control card used in the robot of this experimental platform. Using the interface provided by the control card, the TCP/IP communication protocol is used to enable the host computer to send angle data to the control card, thus realizing the motion control of the robot.

GALIL motion control card provides a wealth of robot motion control function interface, according to the needs of this experimental platform, in the host computer to complete the image acquisition and feature extraction to get the image plane error, and then the use of non-calibrated visual servo algorithms to calculate the robot joints incremental angle, then, only need to send the angle incremental to the control card, so that the control card to control the robot movement can be. The main functions used in this experiment are the multi-axis relative motion instruction, which lets the specified joint motors move a given number of pulses relative to the current position. The number of pulses n is calculated by equation (15):

$$n = \Delta\theta \frac{\gamma \cdot \delta}{2\pi} \tag{15}$$

where $\Delta\theta$ is the angular increment calculated by the algorithm, and γ, δ is the resolution of the motors and the reduction ratio of the robot joints, respectively.

2.2. Deep Learning Based Image Jacobi Matrix Model Construction

2.2.1. Kalman Filtered Image Jacobi Matrix

Currently, the image Jacobi matrix is one of the most widely used hand-eye mapping relationship models in the field of robot vision servoing. The image Jacobi matrix model was first proposed by Weiss and is defined as follows:

$$\dot{f} = J_i(r) \cdot \dot{r}$$

$$J_i(r) = t\left(\frac{\partial f}{\partial r}\right) = t\left(\begin{bmatrix} \frac{\partial f_1(r)}{\partial r_1} & \cdots & \frac{\partial f_1(r)}{\partial r_n} \\ \vdots & \ddots & \vdots \\ \frac{\partial f_m(r)}{\partial r_1} & \cdots & \frac{\partial f_m(r)}{\partial r_m} \end{bmatrix}_{m \times n}\right) \tag{16}$$

where $f \in R^m$ is the image feature parameter vector, representing m image feature parameters, $r \in R^n$ is the coordinate parameter of the robot's end in the task space, and $J_i(r) \in R^{m \times n}$ is the image Jacobian matrix, which reflects the differential mapping relationship between the robot's movement space and the differential mapping relationship between the robot motion space and the image feature space, also known as the interrelationship matrix, B-matrix.

Since the control quantity of a part of the robot system is the joint motion velocity, it is necessary to establish a differential mapping relationship between the joints and the ends of such systems:

$$\dot{r} = J_r \cdot \dot{q} \tag{17}$$

where $\dot{q} \in R^p$ is the velocity vector of motion in the p -dimensional robot joint space. $\dot{r}$ is the end velocity of the robot in the robot's task space, and J_r , often called the robot Jacobi matrix, represents the mapping relationship between the robot's joint velocities to the end velocities in the following form:

$$J_r = t\left(\frac{\partial r}{\partial q}\right) = t\left(\begin{bmatrix} \frac{\partial r_1}{\partial q_1} & \cdots & \frac{\partial r_1}{\partial q_n} \\ \vdots & \ddots & \vdots \\ \frac{\partial r_n}{\partial q_1} & \cdots & \frac{\partial r_n}{\partial q_n} \end{bmatrix}\right) \tag{18}$$

Combining the robot Jacobi matrix equation (18) and the visual projection mapping transformation equation (16), the relationship between the robot joint motion velocity and the image feature motion velocity can be obtained:

$$\dot{f} = J_i \cdot \dot{r} = J_i J_r \cdot \dot{q} \tag{19}$$

Let $J = J_i J_r$, Eq. (19) can be simplified to the mapping relationship shown in Eq. (20). A mapping model from the robot joint motion space to the image feature space is established:

$$\dot{f} = J \cdot \dot{q} \tag{20}$$

Up to this point, a direct mapping from the robot joint space to the image space, i.e., the overall Jacobi matrix of the camera-robot system, has been established. This matrix directly reflects the proportionality between the robot's joint motion in the current state and the corresponding image feature changes, based on which various image feedback controllers can be constructed. The image Jacobi matrix is related to the parameters inside and outside the camera and varies with the robot end motion, so it needs to be estimated in real time. In addition, what is usually needed in the control system is an inverse mapping relation of the image Jacobi matrix, which is because the goal of feedback control is to compute the robot end motion $\dot{r}$ or joint motion $\dot{q}$ based on the motion of the image features $\dot{f}$. This inverse mapping relation can be equated to the problem of inverting the Jacobi matrix.

2.2.2. Kalman Filter Theory

The core of direct visual servo control through online recognition of the image Jacobi matrix is the online recognition algorithm, and the result of the recognition algorithm determines the system control effect. Since the uncalibrated servo control system has no parameter information of the model, the estimation algorithm must make full use of the robot's own motion and the image information obtained from the camera to estimate the image Jacobi matrix. Since the Jacobi matrix changes continuously with

the motion of the robot, the estimation algorithm must be able to be synchronized in the control process, which has certain requirements for real-time. Moreover, the estimation algorithm also needs some filtering ability because the state variables and output variables of the system contain noise pollution. According to the state space model of discrete system, a discrete linear dynamic system can be described as:

$$x_k = F_k x_{k-1} + B_k u_k + w_k \tag{21}$$

$$z_k = H_k x_k + v_k \tag{22}$$

In Eq. (21), x_k is the state of the system at the moment k, and u_k is the control quantity input to the system at the moment k. F_k is the state transformation matrix acting on the state x_{k-1} at the previous moment, B_k is the matrix acting on the current input vector u_k to the controller, and w_k is the process noise, assuming $w_k \sim N(0, Q_k)$, and Q_k is the covariance matrix of the multivariate normal distribution. Equation (22) represents the relationship between an observation z_k of the true state x_k and the state for any moment k. Where H_k is the observation matrix, which maps the true state space of the system to the observation space to obtain the observed quantities, and v_k is the observation noise, which is assumed to satisfy $v_k \sim N(0, R_k)$. Also, assume that the initial state and the noise at each moment $\{x_0, w_1, ...w_k, v_1, ...v_k\}$ are independent. It can be seen that the Kalman filter actually contains many assumptions, and therefore many real systems do not exactly fit its model [24]. However, an approximate Kalman filter model can also provide a good simulation of the real system since it takes into account the noise interference.

The two phases of the Kalman filtering method are described below.

(1) Prediction phase. In the prediction phase, the filter makes a prediction of the current state based on the state of the previous moment and the system transformation matrix. The state of the Kalman filter contains two elements $\hat{x}_{k|k}$ and $P_{k|k-1}$. $\hat{x}_{k|k}$ is the state estimate at the k moment, and $P_{k|k-1}$ is the covariance of the estimation error (or covariance matrix in multivariate case), which represents the error between the estimated value and the true value, and is used as a measure of the accuracy of the estimate. According to the system model, the state of the system at the next moment can be predicted based on the state of the system at the previous moment, and the prediction process is as follows:

$$\hat{x}_{k|k-1} = F_k \hat{x}_{k-1|k-1} + B_k u_k \tag{23}$$

$$P_{k|k-1} = F P_{k-1|k-1} F^T + Q_k \tag{24}$$

where $\hat{x}_{k|k-1}$ is the predicted value based on the state at the previous moment, $\hat{x}_{k-1|k-1}$ is the optimal estimation of the state at the previous moment, u_k is the control quantity for the current state, $P_k \mid k-1$ is the $\hat{x}_{k|k-1}$ corresponding to the covariance, and $P_{k-1|k-1}$ is the covariance corresponding to $\hat{x}_{k-1|k-1}$.

(2) Update phase. After the prediction process, the prediction result is obtained. The filter combines the prediction results with the measurements at the current moment and calculates the optimal estimate $\hat{x}_{k|k}$ and the covariance matrix $P_{k|k}$ at the current moment based on the Kalman gain. First the Kalman gain matrix needs to be computed:

$$K_k = P_{k|k-1} H_k^T (H_k P_{k|k-1} H_k^T + R_k)^{-1} \tag{25}$$

Next, the optimal estimate and covariance matrix at moment k are computed based on the Kalman gain:

$$\hat{x}_{k|k} = \hat{x}_{k|k-1} + K_k (z_k - H_k \hat{x}_{k|k-1}) \tag{26}$$

$$P_{k|k} = (I - K_k H_k) P_{k|k-1} \tag{27}$$

2.2.3. Online Estimation of the Image Jacobi Matrix

Using the image Jacobi matrix to describe the hand-eye mapping relationship is essentially approximating a nonlinear time-invariant system to a time-varying linear system, so estimating the Jacobi matrix is equivalent to estimating the parameters of this linear time-varying system [25]. According to the previous section, if it is possible to construct a system in which the image Jacobi matrix to be estimated (or a transformation of the Jacobi matrix) is used as the state of the system, the Kalman filtering algorithm can be used to estimate the state of the system. In the process of estimating the state of the system using the Kalman filtering algorithm, the estimated image Jacobi matrix is robust because the filter itself takes into account the effect of noise in the observation of the state of the system. By the definition of image Jacobi matrix:

$$\dot{f} = J(p) \cdot \dot{p} \tag{28}$$

where f is the m-dimensional image feature parameter vector, $\dot{f}$ represents the amount of velocity of the feature in the image feature space, p is the n-dimensional position vector of the end of the dimensional robot in the task space, and $\dot{p}$ represents the velocity of the end of the robot in the task space.

Discretizing this model yields:

$$f(k+1) \approx f(k) + J(p(k)) \cdot \Delta p(k) \tag{29}$$

To realize the estimation of the individual elements of the matrix $J(p)$, $J(p)$ can be transformed into a $mn \times 1$-dimensional observation vector as follows:

$$x = t\left(\frac{\partial f_1}{\partial p} \quad \frac{\partial f_2}{\partial p} \cdots \frac{\partial f_m}{\partial p} \right) \tag{30}$$

where $\frac{\partial f_i}{\partial p} = t\left(\frac{\partial f_i}{\partial p_1} \cdots \frac{\partial f_i}{\partial p_n} \right)^T$ represents the i th row of the Jacobi matrix $J(p)$.

Define the observation vector $x(k)$ obtained from the Jacobi matrix transformation as the state of the system to be estimated, define the state transfer matrix as the unit array $I_{mn \times mn}$ and define the image characteristic motion velocity as the output of the system, i.e., $z(k) = f(k+1) - f(k)$, and obtain the state equation of the system as follows:

$$\begin{cases} x(k+1) = x(k) + w(k) \\ z(k) = H(k)x(k) + v(k) \end{cases} \tag{31}$$

where $w(k)$ is the state noise and $v(k)$ is the image observation noise, and they are both assumed to be Gaussian white noise.

$$H(k) = \begin{bmatrix} \Delta p(k)^T & \cdots & 0 \\ \vdots & \ddots & \vdots \\ 0 & \cdots & \Delta p(k)^T \end{bmatrix}_{m \times mn} \tag{32}$$

Based on the Kalman algorithm described in Eqs. (23) to (26), the following recursive estimation is established:

$$\hat{x}^-(k) = \hat{x}(k-1) \tag{33}$$

$$P(k) = P(k-1) + Q_k \tag{34}$$

$$K(k) = P(k)H(k)^T (H(k)P(k)H(k)^T + R_k)^{-1} \tag{35}$$

$$\hat{x}(k) = \hat{x}^-(k) + K(k)(z(k) - H(k)\hat{x}^-(k)) \tag{36}$$

$$P(k) = (I - K(k)H(k))P(k) \tag{37}$$

Where Q_k, R_k is the noise covariance matrix, which needs to be set according to the noise situation in the actual environment. $P(k)$ is the state estimation error covariance matrix, generally its initial value can be taken as $P(0) = 10^5 \cdot I_m$ (I_m refers to the m dimensional unit array). The initial value of the state estimation $\hat{x}(0)$ (in this system, representing the $f(0)$ to be estimated) can be obtained from any n steps of linearly independent trial motion according to the least squares method. This is done by applying n steps of linearly independent trial motions $\Delta p_1, ..., \Delta p_n$ and observing the ensuing change of features in the corresponding image space $\Delta f_1, ..., \Delta f_n$ and then obtain an initial state estimate of the Jacobi matrix according to the following mapping relation:

$$\hat{J}(0) = [\Delta f_1, ..., \Delta f_n] \cdot [\Delta p_1, ..., \Delta p_n]^{-1} \tag{38}$$

Using $\hat{f}(0)$ as $\hat{x}(0)$, only n steps of linearly-independent trial motions are applied to the initial state of the system during each recursive estimation, and the information obtained in the previous tracking motions can be used directly in the subsequent estimation of the Jacobi matrix.

Online estimation of the image Jacobi matrix using Kalman filtering essentially recognizes the system model in real time, allowing for robot tracking by continuously matching and tracking in the image.

2.3. Clothing Structure Design Based on Jacobi Matrix

Clothing process structure template to achieve sewing is realized through certain mechanical principles, the realization of folding, track control, sewing route control realized, free from the dependence on manual skills, directly enhance the production efficiency, and improve the overall quality of the production [26]. This paper is based on the Jacobi matrix optimization algorithm designed in the previous paper to achieve the digital design of the garment structure [27].

2.3.1. Stitch Control in Garment Sewing

The route control of sewing needs to be realized by the slotting of the template, which is to be opened on the sewing position line of the cut pieces. The raised cylinder on the needle plate of the template sewing machine, open in the open slot, the use of Jacobi matrix optimization algorithm, control the sewing track, in the slotted trajectory to obtain effective operation to achieve sewing accuracy, complete high-quality sewing.

2.3.2. Displacement Control in Garment Sewing

In the specific garment sewing process, the cutting piece in the mold through the friction between the template sandpaper to achieve the position fixed control. Therefore, in the design process, the garment cutting piece will not be easy to slide, which can well avoid the sewing will occur in a certain shift problem. In addition, when the upper and lower layers of the cut pieces need a certain degree of elasticity, the corresponding sponge piece can be added between the templates, and at the same time, combined with the trajectory estimation of the Jacobi matrix optimization algorithm, the length of the cut pieces can be effectively controlled.

2.3.3. Clothing Style Recognition

First of all, the application of Jacobi matrix optimization algorithm can accurately capture the visual information contained in the clothing, including clothing patterns, lines, shapes, etc. The designers can use the Jacobi matrix optimization algorithm and image processing technology to extract representative feature vectors. Designers can use the Jacobi matrix optimization algorithm and image processing technology to extract representative feature vectors, which can be used to represent the visual characteristics of various clothing styles, and promote the subsequent style identification and classification work. Jacoby matrix optimization algorithm combined with machine learning algorithms can efficiently identify a variety of clothing styles, designers can use this technology to carry out classification exercises of known styles, machine learning algorithms can learn the characteristic patterns of styles, so as to realize the automatic classification and identification of unknown styles. Secondly, the Jacobi matrix optimization algorithm generates a corresponding dataset, which designers can rely on to obtain images of various styles of clothing, and do a good job of classification and labeling. In addition, the dataset can also train and test the style recognition model, and the change of style information will

also be visualized in the generated samples. Finally, designers use the Jacobi matrix optimization algorithm to successfully carry out model evaluation and continuously improve the design work, in order to analyze the accuracy and stability of the model, designers according to the final evaluation results, effectively grasp the performance of the model and possible problems, and then complete the optimization of apparel design.

3. Structural Design and Wearing Comfort Analysis of Garments

3.1. Detection Results

3.1.1. Subjective Testing of Sample Garments for Inspection

Two different relaxation amounts of test samples of clothing for fitting experimental evaluation, the test results will be substituted into the model, the test results and the results calculated by the model are compared as shown in Table 1 to Table 2.

Table 1 shows the comparison between the actual measured values and the calculated values of the model for the fitted experimental samples, and it can be seen from the numerical values that the values obtained by substituting the scores of individual indicators into the mathematical model do not differ much from the actual measured values, and the difference between the two values is 0.0269, which proves the reasonableness and applicability of the model.

Table 1. The actual measured value of the coating is compared with the model calculation.

Subjective evaluation	Static general sense	Overall comfort					
			Ministries	Back	Chest	Shoulder center	Waist
Model calculation	4.7127	Bend over	3.9248	3.8248	-	-	4.0548
		Forward lift 90°	3.7985	3.7655	-	-	-
		Raise up	3.6425	-	-	-	-
		Lateral raise 45°	3.9963	3.9566	3.7468	-	-
		Sit upright	3.8487	3.8486	3.7398	3.8498	-
Actual measured value	4.7396	3.9265					

Table 2 shows the comparison between the actual measured values and the model calculated values of the fitted experimental sample garment, similarly, the overall comfort is 4.9136, and the model calculated and actual measured values of aesthetics are 4.2348 and 4.3898 respectively, and there is not much difference between the values measured by the model and the actual measured values.

Table 2. The actual measurement and the model calculation of the experimental sample.

Subjective evaluation	Static general sense	Overall comfort					
			Ministries	Back	Chest	Shoulder center	Waist
Model calculation	4.2348	Bend over	4.8582	4.8462	4.8263	4.8264	4.8158
		Forward lift 90°	4.8469	4.8168	-	-	-
		Raise up	4.7251	-	-	-	-
		Lateral raise 45°	5.1365	4.9456	4.4168	4.7485	-
		Sit upright	4.8596	4.8869	-	4.8699	-
Actual measured value	4.3898	4.9136					

3.1.2. Garment Size Estimation Based on Jacobi Matrix Optimization Algorithm

The longitudinal dimensions and elongation of the garments were calculated as shown in Table 3.

Each garment contains a total of three sets of mesh, the mutually symmetrical single-row mesh on the sleeve barrel 1 and sleeve barrel 2 and the staggered three-row mesh on the garment barrel. Since the single row of mesh holes on both the sleeve barrel and the sleeve cylinder are symmetrical in design, the right sleeve barrel and the single row of mesh holes on the right sleeve barrel were selected for the study. The data for the thin-tissue garment were more prominent, with flower height and longitudinal elongation of 1285 transverse columns and 6.4251%, respectively.

Table 3. The vertical size and elongation of the garment.

Clothing	Copper sheet	Flower height/horizontal column	Calculate the longitudinal length/cm	Longitudinal length /cm	Longitudinal elongation/%
Thin tissue Clothes	Jacket barrel	1090	39.7485	39.7485	0
	Sleeve	1285	47.8612	50.5315	6.4251
Thick tissue Clothes	Jacket barrel	1090	53.5425	53.5314	0
	Sleeve	1030	50.5365	50.5987	0

3.2. Clothing Comfort Analysis

3.2.1. Subjective Comfort

The five experimental samples of pants are the best-selling pants in the market, which are numbered 1#, 2#, 3#, 4#, and 5#, respectively. 1# is the normal style, 2# is the style with pockets, and 3#~5# are the pants designed based on the optimization of Jacobi matrix algorithm. Table 4 shows the subjective comfort evaluation of pants wearing.

There was a significant difference (<0.001) in the subjective comfort of the subjects wearing the 5 different pants in the 3 postures. In comparison, 4# had the highest mean comfort rating of 4.5 and above, which was the best wearing comfort and most recognized by young women. Secondly, 3# and 5# also had higher comfort mean values, ranging from 4.17 to 4.29, with better wearing comfort as well.1# and 2# had average wearing comfort, with an overall evaluation mean score of no more than 3.5.1# was made of ordinary medium-high waist cotton/ammonia material, and 2# added abdominal belt pocket design on the basis of 1#, which were two basic pants that could not satisfy the increasing comfort needs of young consumers.3#, 4#, 5# waistline is slightly higher than 1#, 2#, 3# for the padded models, abdominal hip design, front waist and abdomen lateral increase in the wide layer of lamb protein fleece fabric, fleece layer of emollient polythermal, softer, warmer, better wearing comfort. 4# for the far-infrared models, 3D hip-cup design, the main body of fabric for the regeneration of cellulosic fibers/nylon/cotton, elasticity, the front waist and abdomen, the back of the waist fabrics with far-infrared printing point processing, warm menstruation disperses cold, warm uterus and protect the uterus, the far-infrared printing point processing, the far-infrared printing point processing. Warm menstruation disperses cold, warms the uterus and protects the waist, and is warm and comfortable to wear. 5# is a magnet model, designed to tighten the abdomen and lift the buttocks, the front abdomen and the middle of the back waist are embedded in fabrics with Tomalin magnets, which efficiently releases far-infrared rays, promotes metabolism, improves microcirculation, and the thermal effect of human body absorbing a large amount of far-infrared rays makes the skin temperature rise. It can be seen that the structural optimization by Jacoby Matrix Optimization Algorithm has resulted in better wearing comfort and a relatively higher degree of acceptance.

Table 4. The pants were evaluated with subjective comfort.

Posture	Sample number					F value and its significance
	1#	2#	3#	4#	5#	
Standing	3.4856	3.2152	4.3425	4.6321	4.2985	13.8654***
Sit up	3.5496	3.2985	4.2698	4.5365	4.1326	9.7482***
Total squat	3.3499	3.5698	4.2669	4.4325	4.0948	7.7485***

Note: *** indicates that the correlation coefficient is significant at the 0.001 level.

3.2.2. Pressure Comfort and Distribution

In order to further compare the specifics of wearing comfort of different pants, the subjects' comfort scores of waist, thigh, crotch, buttocks, and overall comfort when wearing each of the 5 pants in 3

postures were plotted into a subjective comfort characteristic graph, and the results are shown in Fig. 2, with the standing posture in Fig. (a), the sitting posture in Fig. (b), and the squatting posture in Fig. (c).

The subjective comfort of young women wearing five different pants in different postures showed their own characteristics with obvious differences. When standing up, the mean values of overall comfort and comfort in each part of the sample pants wearing were ranked as 4# (4.87) > 3# (4.6146) > 5# (4.5392) > 2# (3.5787) > 1# (3.4688). When sitting up straight, the mean values were ranked as 4#>3#>5#>1#>2#, and the subjective comfort scores were 4.7689, 4.321, 4.2887, 2.6011, and 2.1515, respectively.In full squatting, the mean values were ranked as 4#>5#>3#>2#>1#.In all three positions, 4# had the highest comfort in all major parts of the lumbar area, buttocks, thighs, and crotch, as well as the highest subjective overall comfort. 1# and 2# have the highest mean scores, which are most satisfactory to the subjects and meet their needs for wearing comfort. 1# and 2# have mean scores of 2.1-3.6 for wearing comfort, which are generally recognized.

The above analysis shows that 4# has the best overall comfort, and 1# and 2# have relatively poor comfort. 3# and 5# have subjective comfort between the above two. Therefore, 1# and 2#, as basic pants, only satisfy the basic needs of wearing and do not pay more attention to comfort in the design and production. 3#, 4# and 5#, as optimized structural design of the pants, use the fabrics of lamb protein velvet, far-infrared printing dots, and Tomalin magnet and the structure of raising the waistline, tightening the abdomen, and lifting the buttocks to enhance the comfort of wearing, which is generally better than that of the conventional pants.

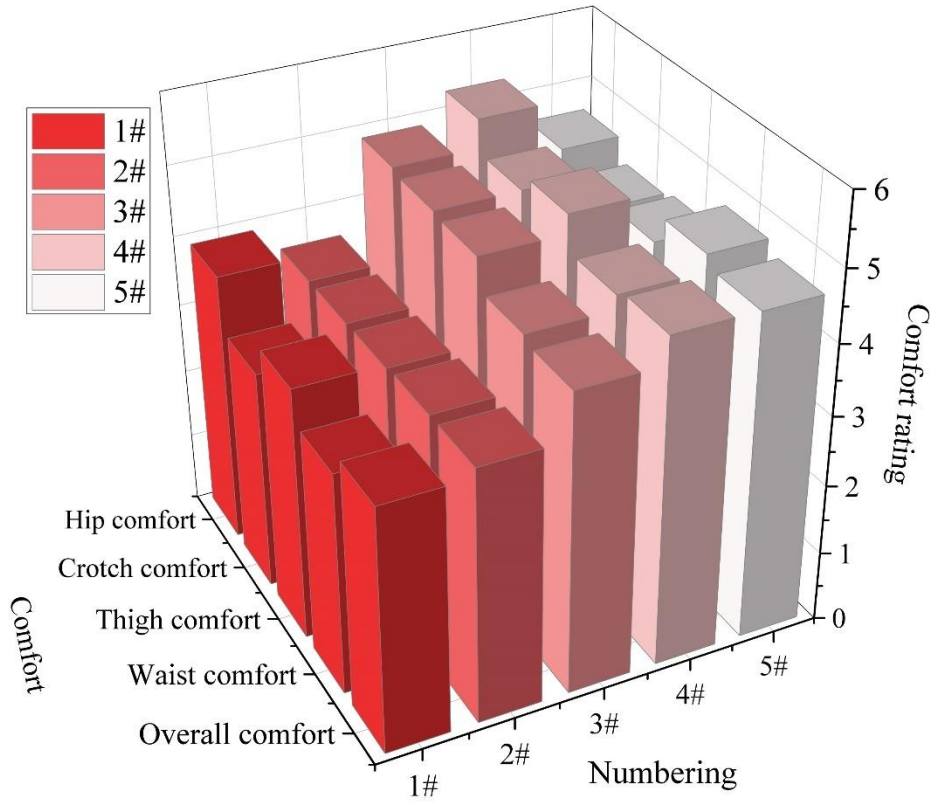

(a) Standing posture

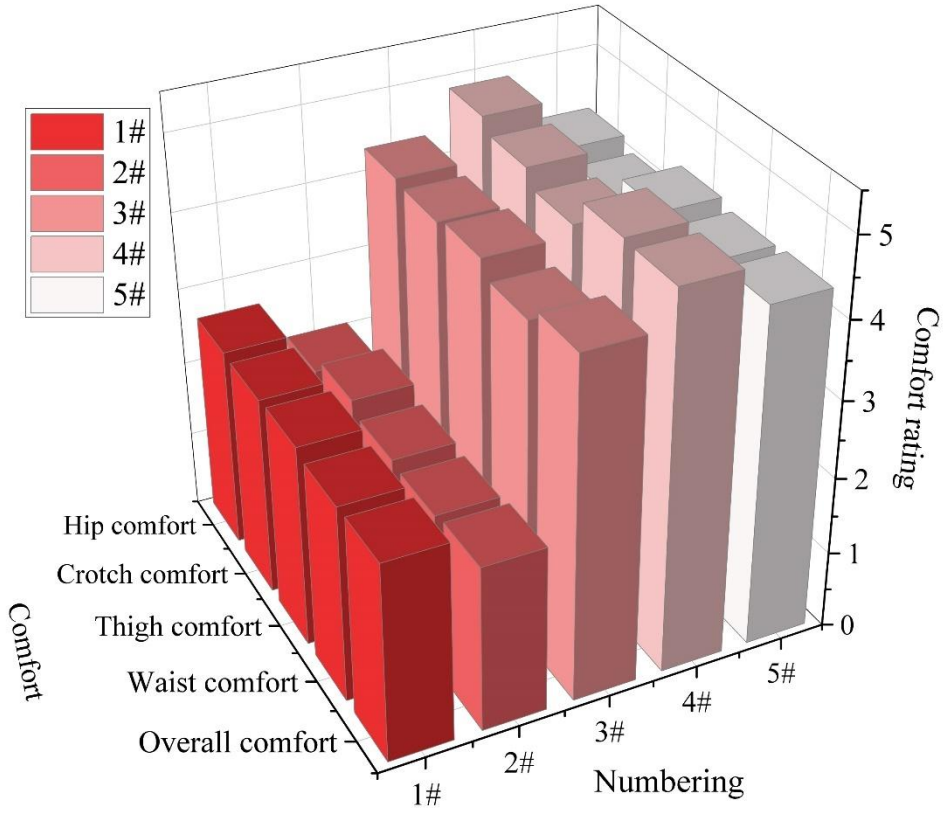

(b) Sitting posture

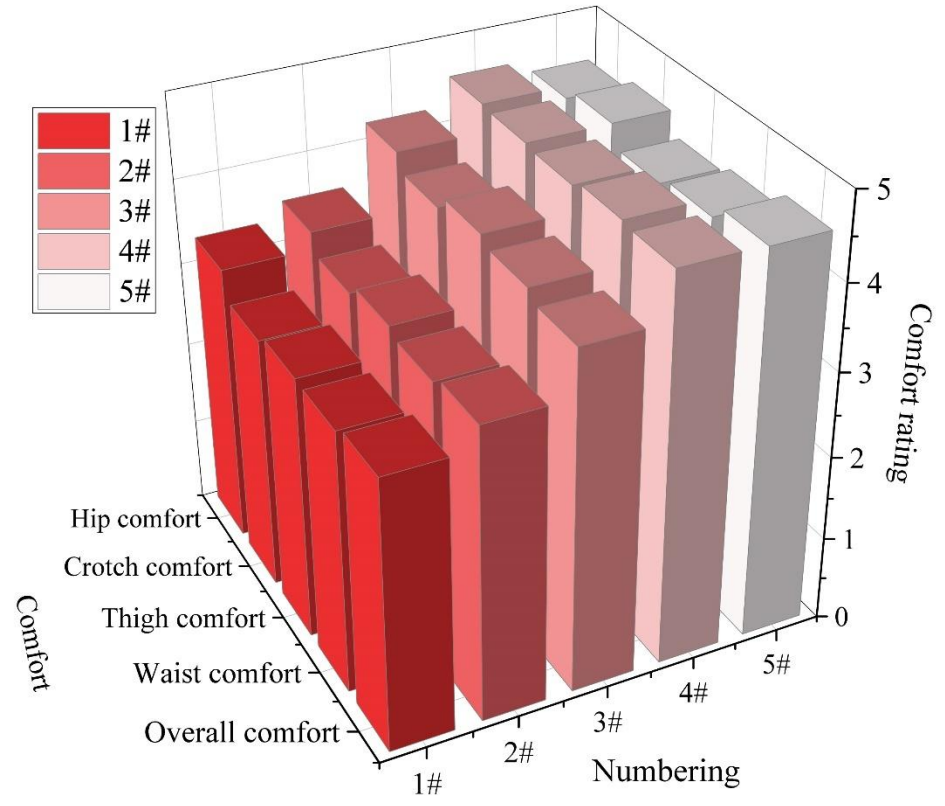

(c) Squatting position

Figure 2. The characteristics of the subjective comfort of trousers under three poses.

Figure 3 shows the pressure distribution of pants in 3 postures, Figure (a) is the standing posture, Figure (b) is the sitting posture, and Figure (c) is the squatting posture, and the wearing of 5 types of pants in 3 postures presented different pressure magnitudes and pressure distributions at each test point. Comparatively speaking, the pressure values at the test points corresponding to the waist (A, B) and crotch (E, F) were lower than those at the test points corresponding to the thighs (C, D, H) and buttocks (G). It can be seen that the 5 sample pants have lower pressure on the body at the waist and crotch than at the thighs and buttocks, which is closely related to the degree of undulation of the body and the skin area. Under different postures, the thigh and hip muscles of the human body will undergo obvious deformation, leading to stretching, folding and other deformations of the clothes worn externally, and the pressure value of the deformed parts is higher than that of the waist and crotch, which are relatively stable.

Among the 5 pairs of pants, 1# has the highest pressure value at point G when standing up, which is 4.4853 kPa, and the pressure value at point G when sitting up straight is also higher, with a pressure value close to 4 kPa. it can be seen that 1# has a greater sense of compression on the buttocks of the human body. 2# has the highest pressure value at point D, which ranges from 4.3764 to 4.573 kPa, and the pressure at the rear middle of the thigh of the pants of 2# has a greater sense of compression on the middle of the back of the thigh of the human body. 3#, 4# and 5# have higher pressure values at each pressure test point than that of the waist and crotch, which are relatively stable, 5# have a lower degree of pressure undulation at each pressure test point than 1# and 2#, and the overall pressure distribution is more balanced. Therefore, 1# is the basic model, 2# added front pocket design under the premise of the basic model, does not have substantial structural optimization, functional design, the overall wearing comfort of these two basic sample pants is a little worse than the functional pants 3#, 4#, 5#.

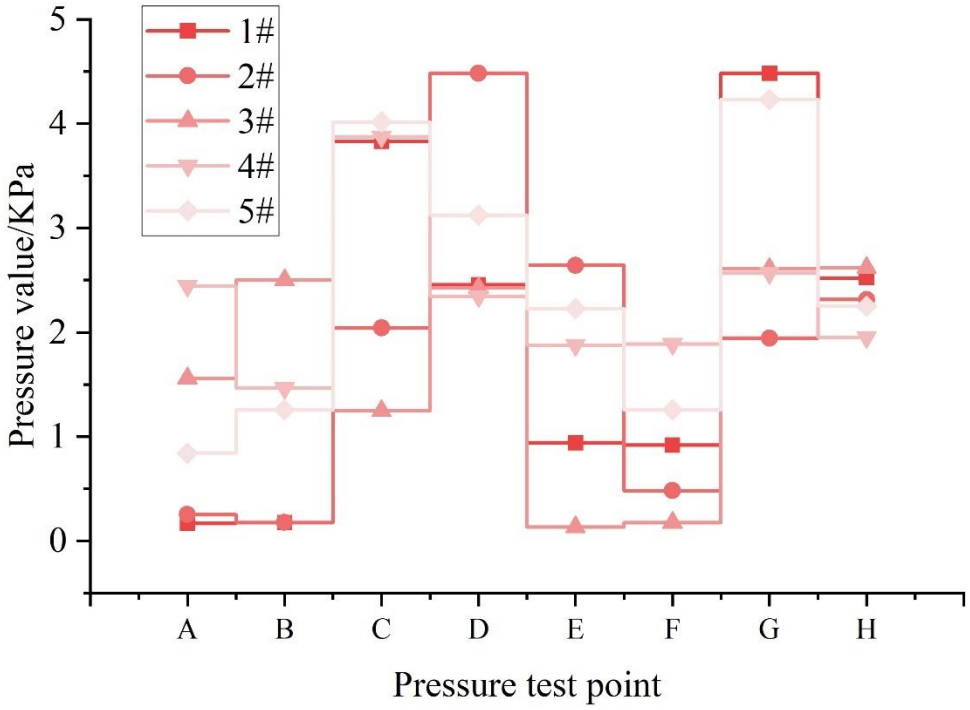

(a) Standing posture

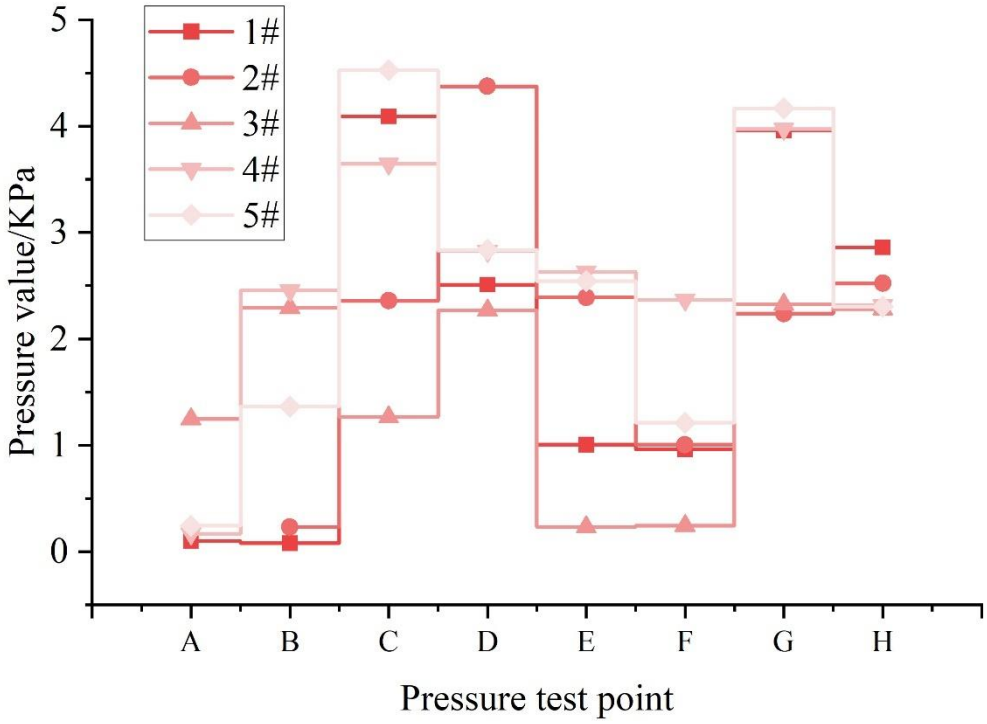

(b) Sitting posture

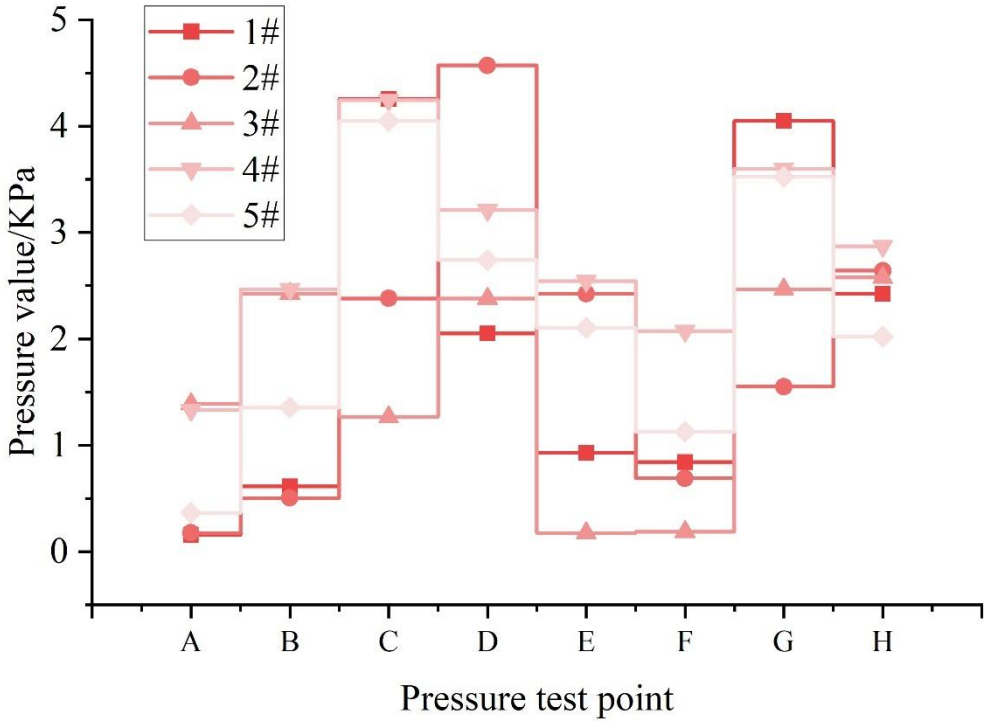

(c) Squatting position

Figure 3. The pressure distribution of trousers under three poses.

3.3. Satisfaction with Clothing Construction

3.3.1. Satisfaction Evaluation of Clothing Local Structure

Comparing the clothing structure satisfaction of the normal model and the optimized model, the normal model is A and the optimized model is B. Significant difference analysis was performed using

ANOVA one-way analysis of variance in SPSS software for the evaluation of satisfaction with the local structure of the clothing, the evaluation of the comfort of the local parts of the body, and the evaluation of the overall satisfaction of the clothing. Significant difference levels of $p<0.05$ (indicated by *) and $p < 0.01$ (indicated by **) were set.

The results of the local structure satisfaction evaluation of the normal and optimized models of clothing are shown in Figure 4. From the figure, it can be seen that the comfort of the optimized model hat, collar, sleeves and cuffs are higher than that of the normal model, and the mean value of the comfort satisfaction of the optimized model sleeves reaches 4.0288, and the mean value of the comfort satisfaction of the hat reaches 4.1548. According to the statistical analysis of all the other parts of the comfort satisfaction evaluations except for the cuffs, there is a significant difference, which indicates that the comfort of the optimized model hat, collar and sleeves have a The comfort of the optimized model hat, neckline and sleeves are all significantly improved, among which the comfort satisfaction evaluation of the sleeves is improved by 0.9019 grades, and the hat and neckline are improved by 2.1103 and 1.2896 grades respectively, which shows a highly significant difference. Although the mean value of comfort satisfaction of the optimized model's cuffs improved by 0.3331 grades compared with that of the normal model, the change in subjective comfort was not significant and did not satisfy the ANOVA chi-square test.

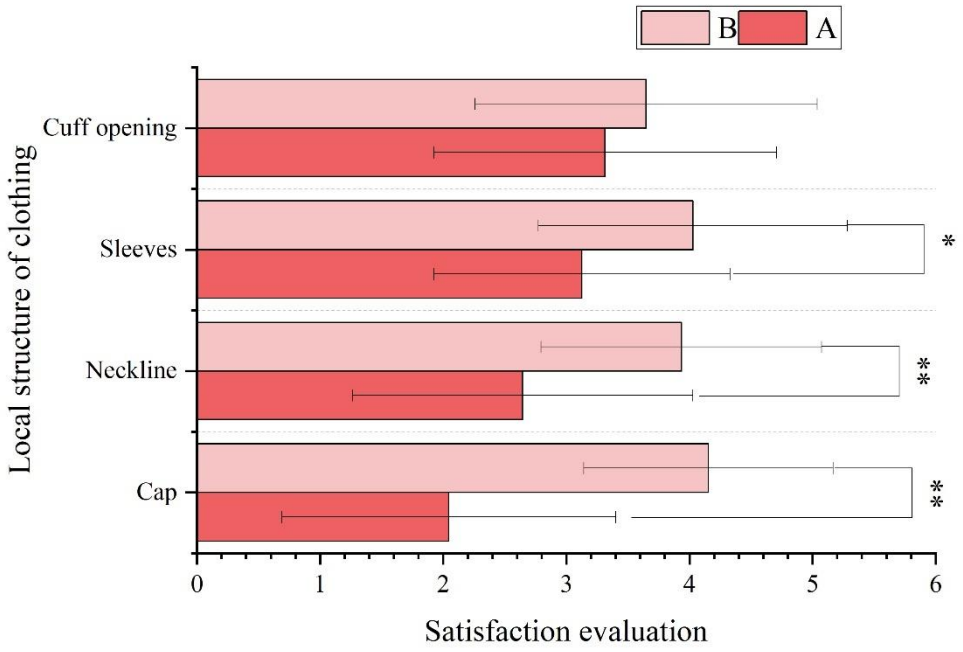

Figure 4. Satisfaction evaluation of the local structure of the clothing.

3.3.2. Evaluation of Comfort in Localized Body Parts

Figure 5 shows the results of the evaluation of the comfort of parts of the body in both regular and optimized garments. Compared with the ordinary model, the average comfort evaluation of the optimized model has been improved, and the average comfort evaluation of the neck and arms of the optimized model has reached more than 4.3, and the average comfort evaluation value of the armpit has reached 4.0298. According to statistical analysis, there were significant differences in the comfort evaluation of other parts except the crotch and buttocks, and the mean comfort evaluations of the neck, armpits, arms and waist increased by 1.2163, 1.0813, 0.9263 and 0.95 grades, respectively, indicating that the comfort of the optimized parts of the local parts has been significantly improved. Compared with the ordinary model, the average comfort evaluation of the crotch and buttocks of the optimized model increased by 0.8437 and 0.553 grades, respectively, and the numerical variance of the comfort evaluation was uneven, and the data did not change significantly, indicating that the comfort improvement effect of the crotch and buttocks was not obvious. According to the feedback of the subjects, when the human body bends over, squats, kneels and other actions, the optimized clothing will still have the phenomenon of crotch tightening and hip tightness, so the improvement of the crotch and buttocks does not make the comfort of the clothing achieve obvious results.

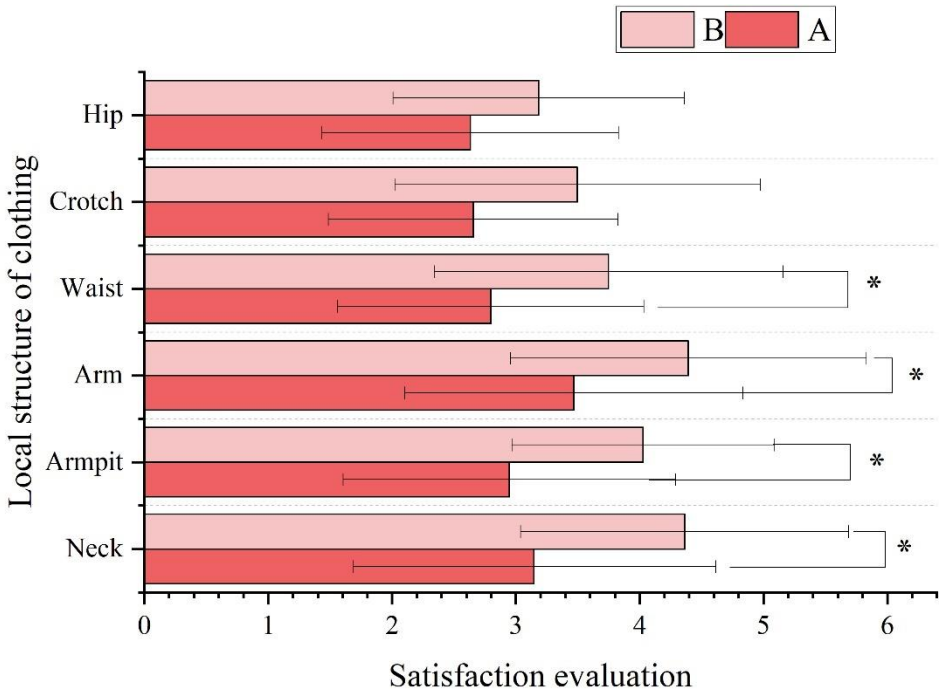

Figure 5. Comfort evaluation of local parts of the body.

3.3.3. Evaluation of Overall Satisfaction with Clothing

The results of the overall satisfaction evaluation of the regular and optimized garments are shown in Figure 6. The satisfaction evaluation mean values of wetness, stuffiness, looseness, ease of movement and overall comfort of the optimized model garments were increased, in which the satisfaction evaluation mean values of ease of movement and overall comfort went up to 4. According to the statistical analysis, the two garments showed highly significant differences in the performance of ease of movement and overall comfort, and their satisfaction evaluation means were increased by 1.4001 and 0.995 grades, while the satisfaction evaluation of wetness, stuffiness and looseness were not varied and did not have significant differences, but their satisfaction evaluation mean values were still improved by 0.45, 0.5498, and 0.2829 grades, respectively, which was mainly due to the improvement of the comfort performance of the localized structural parts, which reduced the subject's discomfort and agitation in wearing the garment and lowered the body's physiological stress response, thus resulting in less sweating and improved satisfaction with the wetness and stuffiness of the garment. On the whole, the improvement of the structural parts of the ordinary garment has significantly enhanced the ease of movement and improved the overall comfort of the garment.

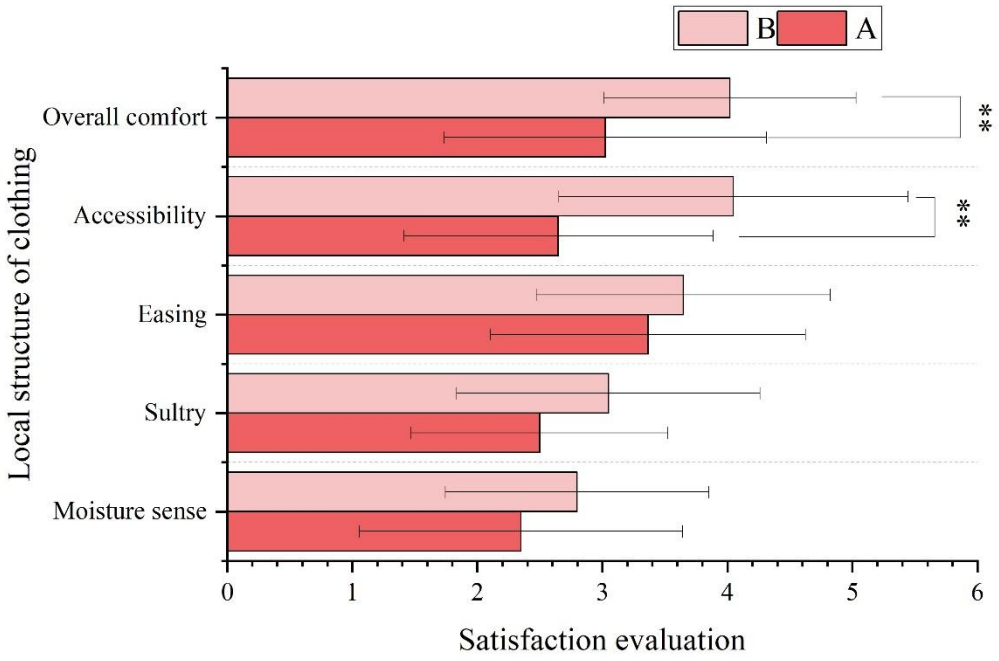

Figure 6. Overall satisfaction evaluation of clothing.

4. Conclusion

In this paper, based on the depth estimation and vision controller, the value of the image Jacobi matrix is calculated to solve the robot end velocity magnitude at the current moment. The image Jacobi matrix is constructed based on Kalman filter to realize the real-time recognition of the system model, and the robot tracking is realized by continuously matching and tracking in the image to control the stitch and displacement control of the garment production.

The test sample garment is evaluated by means of simulation experiments for dressing experiments, and the actual measured values do not differ much from the model estimated values, and in the overall satisfaction, the difference between the two is 0.0269, thus proving the reasonableness and applicability of the model.

For the analysis of the comfort of the clothing, the 4# clothing was improved by the Jacobi matrix optimization design, and the comfort reached 4.5 points and above, with the best wearing comfort and the most recognized by the young women. The distribution of pressure comfort was analyzed for three different postures, and when sitting straight, the mean values were ranked as 4#>3#>5#>1#>2#, and the subjective comfort scores were 4.7689, 4.321, 4.2887, 2.6011, and 2.1515, respectively. It can be seen that 4# has the best overall comfort.

In the overall satisfaction evaluation of the garments, the ease of movement and overall comfort performance of the garments of the normal and optimized models showed highly significant differences, and their satisfaction evaluation mean values were improved by 1.4001 and 0.995 grades, respectively. By improving the structural parts of the normal model garments, the overall comfort of the garments was significantly improved.

References

1. Guo, Z., Zhu, Z., Li, Y., Cao, S., Chen, H., & Wang, G. (2023). AI assisted fashion design: A review. IEEE Access, 11, 88403-88415.
2. Han, S. L., Chan, P. Y., Venkatraman, P., Apeagyei, P., Cassidy, T., & Tyler, D. J. (2017). Standard vs. upcycled fashion design and production. Fashion Practice, 9(1), 69-94.
3. Wei, C., Li, X., Feng, W., Dai, Z., & Yang, Q. (2025). The current research status of Kansei engineering in the field of emotional clothing design. International Journal of Clothing Science and Technology, 37(1), 93-114.
4. Shen, L., & Sethi, M. H. (2021). Sustainable fashion and young fashion designers: Are fashion schools teaching sustainability? Fibres & Textiles in Eastern Europe, 29(5 (149)).
5. Lili, D. A. I., Jiazhen, H. E., Shuai, W. A. N. G., & aofeng, J. I. A. N. G. (2021). Clothing structure design and performance evaluation for long lying people. Wool Textile Journal, 49(1).
6. CHO, El-Lie; KIM, Young-In. A study on meaning of open structure in clothing design. Journal of the Korean Society of Costume, 2006, 56.9: 1-13.

7. XU, Tian-tian; SUN, Ke-ke. Research on the Structure Design of Body Clothing for Elderly Women. In: International Conference on Genetic and Evolutionary Computing. Singapore: Springer Nature Singapore, 2023. p. 398-411.
8. Yue, M. (2016, May). Study on Clothing Structural Design and Modeling. In 2016 2nd Workshop on Advanced Research and Technology in Industry Applications (WARTIA-16) (pp. 251-253). Atlantis Press.
9. LIAO, Jingxiao; HU, Xiaoping. Ergonomics-based clothing structure design for elderly people. In: International Conference on Human-Computer Interaction. Cham: Springer International Publishing, 2021. p. 139-151.
10. Sadkowska, A., Wilde, D., & Fisher, T. (2015). Third age men's experience of fashion and clothing: an interpretative phenomenological analysis. Age, Culture, Humanities: An Interdisciplinary Journal, 2, 35-70.
11. Makkar, M., & Yap, S. F. (2018). The anatomy of the inconspicuous luxury fashion experience. Journal of Fashion Marketing and Management: An International Journal, 22(1), 129-156.
12. Gautam, B., Rijal, H. B., Shukuya, M., & Imagawa, H. (2019). A field investigation on the wintry thermal comfort and clothing adjustment of residents in traditional Nepalese houses. Journal of Building Engineering, 26, 100886.
13. ZHOU, Yueding; ZHU, Hongfeng; CHAO, Yingna. Innovative material applications in clothing design research. Materials Express, 2024, 14.5: 820-827.
14. Yang, C., & Zhang, X. (2023). Environmental protection clothing design and materials based on green design concept. Frontiers in Materials, 10, 1225289.
15. Al-Minyawi, O. M. A., Mahmoud, M. N. I., Ragab, A. G., Al-Gizawy, A. S. H., & Hassabo, A. G. (2025). Smart technology and materials in the clothing industry. Journal of Textiles, Coloration and Polymer Science, 22(1), 171-178.
16. MEI, Wei Yu, et al. An implementation of matrix eigenvalue decomposition with improved Jacobi algorithm. In: 2010 First International Conference on Pervasive Computing, Signal Processing and Applications. IEEE, 2010. p. 952-955.
17. Kautsky, J., & Golub, G. H. (1983). On the calculation of Jacobi matrices. Linear algebra and its applications, 52, 439-455.
18. Wang, Z., Tao, X., Zeng, X., Xing, Y., Xu, Z., & Bruniaux, P. (2023). Design of customized garments towards sustainable fashion using 3D digital simulation and machine learning-supported human–product interactions. International Journal of Computational Intelligence Systems, 16(1), 16.
19. Jin, P., Fan, J., Zheng, R., Chen, Q., Liu, L., Jiang, R., & Zhang, H. (2023). Design and research of automatic garment-pattern-generation system based on parameterized design. Sustainability, 15(2), 1268.
20. Kulińska, M., Abtew, M. A., Bruniaux, P., & Zeng, X. (2022). Block pattern design system using 3D zoning method on digital environment for fitted garment. Textile Research Journal, 92(23-24), 4978-4993.
21. CICHOCKA, Agnieszka; BRUNIAUX, Pascal; KONCAR, Vladan. Modelling of virtual garment design in 3D. Research Journal of Textile and Apparel, 2007, 11.4: 55-63.
22. Li, C. (2024, September). Research on the Development of 3D Garment Virtual Design. In 2024 3rd International Conference on Artificial Intelligence and Computer Information Technology (AICIT) (pp. 1-4). IEEE.
23. José M. A. Matos,Paulo B. Vasconcelos & José A. O. Matos. (2024). On Fourier Series in the Context of Jacobi Matrices. Axioms,13(9),581-581.
24. Yiyuan Ding & Zhenrui Peng. (2025). An improved Dual Kalman Filter method for structural response reconstruction with adaptive noise covariance adjustment. Structures,78,109288-109288.
25. Xinmei Wang,Zhenzhu Liu,Feng Liu & Leimin Wang. (2021). The Estimation of Image Jacobian Matrix with Time-Delay Compensation:Regular papers. Journal of Advanced Computational Intelligence and Intelligent Informatics,25(6),982-988.
26. Yonggang Wang. (2022). Research on the Interpretative Space and Meaningful Structure of "National Trend" Clothing Design. Frontiers in Art Research,4(14),
27. Zhao Qing. (2024). Simulation of 3D digital design of clothing fabrics based on optical imaging detection and image acquisition. Optical and Quantum Electronics,56(4).